

Linear and Nonlinear Analysis of Plain Journal Bearings Lubricated With Couple Stress Fluid

^{#1}Deepali Kangude

¹deepalikangude94@gmail.com

¹P.G. student Mechanical Department, DYPIET Pimpri, Pune,



ABSTRACT

A journal bearing is used to support radial loads under high speed operating conditions. In a journal bearing, pressure is generated in the thin lubricant oil film that separates the shaft and the journal, thus preventing metal to metal contact. In conventional bearing design that lubricant oil film is assumed as Newtonian fluid but in recent years there has been a considerable amount of interest in the lubricating effectiveness of non-Newtonian fluids. Lubricants show the strong influence on the performance of bearing. A lubricant without additives does not serve satisfactorily under general operating conditions. Hence additives are added to lubricant to improve its desired characteristics. Generally additives of organic compounds containing long molecular chain length such as hyaluronic acid, fatty acid and their derivatives as metallic soap, long chain alcohols and organic phosphates which converts the lubricant into couple stress fluid. Hence couple stress in the fluid arises due to presence of additives causing the working fluid to behave as non-Newtonian polar fluid.

The aim of the present dissertation is to evaluate the performance characteristics along with the linear and nonlinear trajectories of a plain circular journal bearing hydrodynamically lubricated with couple stress fluid. Couple stress fluid model based upon the theory of microcontinuum is a most realistic and adequate model to represents a lubricant with additives and contaminants. Present work is foremost categorized into two main modules: a) Linear study b) Nonlinear study

Linear study of journal bearing system includes the determination and analysis of various bearing characteristics. Bearing characteristics includes both static and dynamic type characteristics i.e. attitude angle, bearing force, stiffness and damping coefficients of hydrodynamic journal bearings. Non linear study does not require determination of bearing characteristics. Hence analysis is carried out by calculating static forces and instantaneous fluid film forces. Non linear study includes the determination of critical mass.

Keywords— Couple stress fluid, Hydrodynamic journal bearing, linear and non linear analysis, Modified Reynolds equation, Stokes microcontinuum theorem.

ARTICLE INFO

Article History

Received : 18th November 2015

Received in revised form :

19th November 2015

Accepted : 21st November , 2015

Published online :

22nd November 2015

I. INTRODUCTION

A bearing is a machine element which supports another moving machine element (known as journal) it permits relative motion between the contact surfaces of the members. A little consideration will show that due to the relative motion between the contacting surfaces certain amount of

the power is lost due to friction in overcoming frictional resistance and if rubbing surfaces are in direct contact, there will be rapid wear. In order to reduce the wear, frictional resistance and frictional heat generated, a layer of fluid (known as lubricant) may be provided. The lubricants used are mineral oils which are obtained by refining silicon oil, grease, petroleum etc. Hence bearings are used to prevent

friction between parts during relative movement. In machinery they fall into two primary categories: anti-friction or rolling element bearings and sliding contact bearings. The primary function of a bearing is to carry load between a rotor and the case with as little wear as possible. This bearing function exists in almost every occurrence of daily life such as wrist-watch, automobile, disk drive in computers, robotics, electrical appliances etc. In industry, the use of journal bearings is specialized for both low and high speed rotating machinery. Lubricant introduces stiffness and damping characteristics in journal bearing system. These characteristics plays vital role in reducing the vibration characteristics of machinery. The types of machinery we are concerned with range from small high speed spindles to motors, blowers, compressors, fans, and pumps to large turbines and generators to some paper mill rolls and other large slow speed rotors. A number of studies are carried out using Stokes microcontinuum theory to investigate the effects of the couple stress parameter, 'l', on the performance of different types of fluid film bearings. These studies include work done by Lin [7-10] and hydrostatic thrust bearings by R.S Gupta [4]. The characteristics of pure squeeze film bearings has been analyzed by Ramanaiah and Sarkar[1], and slider bearings are also studied by Ramanaiah [2]. N. B. Naduvinamani and S.B. Patil found the Numerical solution for finite modified Reynolds equation for couple stress squeeze film lubrication of porous journal bearings[13]. It has been noticed that literature concerning the stability of plain circular hydrodynamic journal bearings is available only for the Newtonian fluids and no information is available dealing with the use of couple stress fluids.

The present study is concerned with the stability analysis of a hydrodynamically lubricated plain circular journal bearing. Results are obtained for the analysis of plain circular bearing characteristics lubricated with couple stress fluid with varying couple stress parameter from 0 to 0.5 with the step of 0.1. The effect of eccentricity ratio is also considered by varying it from 0.3 to 0.7 with step size of 0.1.

II. ANALYSIS

A. Basic Equations

In the present study it is assumed that the working lubricant is incompressible couple stress fluid. Modified Reynolds equation is derived for couple stress fluid on the basis of Stokes microcontinuum theorem. On solving continuity equation (expresses conservation of masses) by using solutions of the modified Navier-Stokes equation (expresses conservation of linear momentum).[7]

Continuity equation for three dimensional fluid flows is given by,

$$\frac{\partial \rho}{\partial t} + \nabla \cdot (\rho V) = 0 \quad (1)$$

Modified Navier-stokes equation for incompressible couple stress fluid can be given as

$$\rho A = -\nabla p + \rho F^* + \frac{1}{2} \text{curl}(\rho T) + \mu \nabla^2 V - \eta \nabla^4 V \quad (2)$$

where V , A , F^* and T are the velocity vector, acceleration, body force per unit mass and body couple per unit mass respectively. ρ is the density, p is the hydrodynamic pressure, μ is the shear viscosity and η is a new material

viscosity defining the couple stress property having the units of momentum.

For fluid flow along X-direction,

$$\rho \frac{Du}{dt} = -\frac{\partial p}{\partial x} + \rho f_x + \frac{1}{2} \frac{\partial(\rho T)}{\partial x} + \mu \left(\frac{\partial^2 u}{\partial x^2} + \frac{\partial^2 u}{\partial y^2} + \frac{\partial^2 u}{\partial z^2} \right) - \eta \left(\frac{\partial^4 u}{\partial x^4} + \frac{\partial^4 u}{\partial y^4} + \frac{\partial^4 u}{\partial z^4} \right) \quad (3)$$

For fluid flow along Y-direction,

$$\rho \frac{Dv}{dt} = -\frac{\partial p}{\partial y} + \rho f_y + \frac{1}{2} \frac{\partial(\rho T)}{\partial y} + \mu \left(\frac{\partial^2 v}{\partial x^2} + \frac{\partial^2 v}{\partial y^2} + \frac{\partial^2 v}{\partial z^2} \right) - \eta \left(\frac{\partial^4 v}{\partial x^4} + \frac{\partial^4 v}{\partial y^4} + \frac{\partial^4 v}{\partial z^4} \right) \quad (4)$$

For fluid flow along Z-direction,

$$\rho \frac{Dw}{dt} = -\frac{\partial p}{\partial z} + \rho f_z + \frac{1}{2} \frac{\partial(\rho T)}{\partial z} + \mu \left(\frac{\partial^2 w}{\partial x^2} + \frac{\partial^2 w}{\partial y^2} + \frac{\partial^2 w}{\partial z^2} \right) - \eta \left(\frac{\partial^4 w}{\partial x^4} + \frac{\partial^4 w}{\partial y^4} + \frac{\partial^4 w}{\partial z^4} \right) \quad (5)$$

where u , v and w are the velocity components along X, Y and Z directions respectively. The total derivatives of velocity components $\frac{Du}{dt}$, $\frac{Dv}{dt}$ and $\frac{Dw}{dt}$ are the three components of acceleration of fluid.

In order to simplify the equation following assumptions are made as

1. The fluid is incompressible.
2. For incompressible fluid ρ is constant.
3. The viscosity of lubricant is constant throughout the film.
4. The pressure does not vary across the film. Thus $\frac{\partial p}{\partial z} = 0$.
5. Inertia and body force terms are negligible as compared with the pressure and viscous terms.
6. There is no slip between fluid and solid boundaries.
7. The flow is viscous and laminar.
8. Due to the geometry of fluid film the derivatives of u and w with respect to y are much larger than other derivatives of velocity components. $\frac{\partial u}{\partial y}, \frac{\partial w}{\partial y} \gg \gg$ Other partial derivative terms
So, other partial derivatives can be neglected
9. The height of the film is very small compared to bearing length.

Considering thin incompressible fluid film between journal bearing which leads to absence of body couple, body force and inertia force equation (2) can be written as,

Fluid flow along X-direction,

$$\eta \frac{\partial^4 u}{\partial x^4} - \mu \frac{\partial^2 u}{\partial x^2} = -\frac{\partial p}{\partial x} \quad (7)$$

For fluid flow along Y-direction,

$$\eta \frac{\partial^4 v}{\partial x^4} - \mu \frac{\partial^2 v}{\partial x^2} = -\frac{\partial p}{\partial y} \quad (8)$$

For fluid flow along Z-direction,

$$\frac{\partial p}{\partial z} = 0 \quad (9)$$

The no slip boundary conditions for the velocity distributions are

$$\left. \begin{aligned} \text{At } y = 0; u = 0; w = 0; \\ \text{At } y = h; u = U; w = 0; \end{aligned} \right\} \quad (10)$$

Velocity due to squeeze action of fluid film,

$$v(x, 0, z) = 0, v(x, h, z) = V \tag{11}$$

Couple stress vanishes at the boundary,

$$\frac{\partial^2 u}{\partial z^2} \Big|_{z=0} = \frac{\partial^2 v}{\partial z^2} \Big|_{z=0} = \frac{\partial^2 u}{\partial z^2} \Big|_{z=h} = \frac{\partial^2 v}{\partial z^2} \Big|_{z=h} = 0 \tag{12}$$

Velocity component obtained are:

$$u = U + U \frac{y}{h} + \frac{1}{2\mu} \frac{\partial p}{\partial x} y^2 - \left\{ y^2 - yh + 2l^2 \left[1 - \cosh\left(\frac{2y-h}{2l}\right) X \left(\cosh\left(\frac{h}{2l}\right)\right)^{-1} \right] \right\} \tag{13}$$

$$w = \frac{1}{2\mu} \frac{\partial p}{\partial z} y^2 - \left\{ y^2 - yh + 2l^2 \left[1 - \cosh\left(\frac{2y-h}{2l}\right) X \left(\cosh\left(\frac{h}{2l}\right)\right)^{-1} \right] \right\} \tag{14}$$

Here $l = \sqrt{\frac{\eta}{\mu}}$ U, V are tangential and normal velocity components of journal.

q_x and q_z are along the flow fluxes along X and Z directions. They are given as:

$$q_x = \int_0^h u dy = \frac{U}{2} h - \frac{h^3}{12\mu} f(l, h) \frac{\partial p}{\partial x} \tag{15}$$

$$q_z = \int_0^h w dy = -\frac{h^3}{12\mu} f(l, h) \frac{\partial p}{\partial z} \tag{16}$$

Where $f(l, h) = h^3 - 12hl^2 + 24l^3 \tanh\left(\frac{h}{2l}\right)$

Modified Reynolds equation governing the pressure distribution on the film is given as,

$$\frac{\partial}{\partial x} \left\{ f(l, h) \frac{\partial p}{\partial x} \right\} + \frac{\partial}{\partial z} \left\{ f(l, h) \frac{\partial p}{\partial z} \right\} = 6\mu U \frac{\partial h}{\partial x} + 12\mu \frac{\partial h}{\partial t} \tag{17}$$

B. Non-Dimensional Form of Modified Reynolds Equation

The non-dimensional form of modified Reynolds equation for an incompressible fluid with couple stress is obtained on substituting:

$$\theta = \frac{x}{R_j}; \bar{h} = \frac{h}{c}; \bar{z} = \frac{z}{R_j}; \bar{p} = \frac{pc^2}{\mu UR_j}; \bar{l} = \frac{l}{c}; \omega = \frac{U}{R_j}; \bar{t} = \omega t$$

On substituting non-dimensional values in equation (17) we get,

$$\frac{\partial}{\partial \theta} \left(f(\bar{l}, \bar{h}) \frac{\partial \bar{p}}{\partial \theta} \right) + \frac{\partial}{\partial \bar{z}} \left(f(\bar{l}, \bar{h}) \frac{\partial \bar{p}}{\partial \bar{z}} \right) = 6 \frac{\partial \bar{h}}{\partial \theta} + 12 \frac{\partial \bar{h}}{\partial \bar{t}} \tag{18}$$

where $f(\bar{l}, \bar{h}) = \bar{h}^3 - 12\bar{h}\bar{l}^2 + 24\bar{l}^3 \tanh\left(\frac{\bar{h}}{2\bar{l}}\right)$

C. Film Thickness

Schematic figure of plain circular bearing is shown in Figure 1 below. Wedge film is formed due to curved surface of journal and bearing. Following equation gives non-dimensional fluid film formed at the location from positive Y axis:

$$\bar{h} = 1 - \bar{X}_j \cos(90 + \phi + \theta) - \bar{Y}_j \sin(90 + \phi + \theta) \tag{19}$$

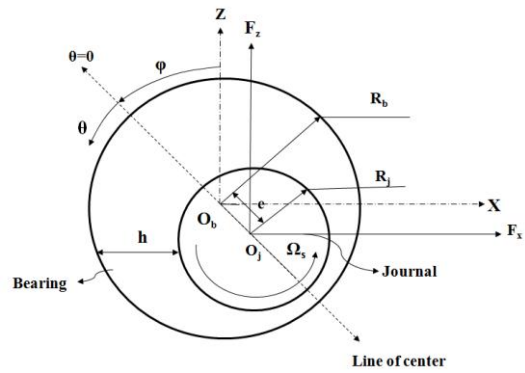


Fig.1 Schematic diagram of a plain circular journal bearing

D. Load Carrying Capacity

Following expressions gives vertical and horizontal components of load,

$$\bar{F}_x = \int_0^{L/R_j} \int_0^{2\pi} \bar{p} \cos(\theta + \phi) d\theta d\bar{z} \tag{20}$$

$$\bar{F}_z = \int_0^{L/R_j} \int_0^{2\pi} \bar{p} \sin(\theta + \phi) d\theta d\bar{z} \tag{21}$$

Resultant load is given as:

$$\bar{F} = \sqrt{\bar{F}_x^2 + \bar{F}_z^2}$$

E. Stiffness Characteristics

In order to find stiffness as one of the bearing characteristics journal is given perturbation (displacement) from its equilibrium position. Given disturbance leads to variation in fluid film thickness and it causes variation in the static equilibrium forces and instantaneous fluid film forces. This variation is used to calculate stiffness coefficients and these are obtained as:

$$\begin{bmatrix} K_{xx} & K_{xz} \\ K_{zx} & K_{zz} \end{bmatrix} = \begin{bmatrix} -\frac{\partial}{\partial \bar{x}} \\ -\frac{\partial}{\partial \bar{z}} \end{bmatrix} [\bar{F}_x \bar{F}_z] \tag{22}$$

The first subscript denotes the direction of force and the second subscript denotes the direction of displacement.

F. Damping Characteristics

To obtain damping characteristics journal perturbation is given in the form of velocity. This disturbance results change in film thickness and force variation in observed between static equilibrium forces and instantaneous forces. These differences in these forces are used to calculate damping coefficient. Hence damping coefficient is given by following equation,

$$\begin{bmatrix} C_{xx} & C_{xz} \\ C_{zx} & C_{zz} \end{bmatrix} = \begin{bmatrix} -\frac{\partial}{\partial \dot{\bar{x}}} \\ -\frac{\partial}{\partial \dot{\bar{z}}} \end{bmatrix} [\bar{F}_x \bar{F}_z] \tag{23}$$

The first subscript denotes the direction of force and the second subscript denotes the direction of velocity.

G. Linear Equations of Motion

By using dynamic characteristics of bearing linear equation can be formulated. Linear equations contain stiffness and damping characteristics and corresponding displacement and velocity components. Set of linear equations are given as:

$$\begin{cases} \bar{M}_j \ddot{\bar{x}} + \bar{C}_{xx} \dot{\bar{x}} + \bar{C}_{xz} \dot{\bar{z}} + \bar{K}_{xx} \bar{x} + \bar{K}_{xz} \bar{z} = 0 \\ \bar{M}_j \ddot{\bar{z}} + \bar{C}_{zx} \dot{\bar{x}} + \bar{C}_{zz} \dot{\bar{z}} + \bar{K}_{zx} \bar{x} + \bar{K}_{zz} \bar{z} = 0 \end{cases} \tag{24}$$

In order to obtain response the journal centre linear study, linear equations motions are solved. Solution of equation (24) is obtained by simultaneous integration using Runge-Kutta 4th order method.

H. Non-Linear Equations of Motion

Non-linear equation of motion is formulated by using journal mass and force gradient between static equilibrium forces and instantaneous forces. Set of nonlinear equations predicting journal centre trajectories are given as:

$$\begin{bmatrix} \bar{M}_j & 0 \\ 0 & \bar{M}_j \end{bmatrix} \begin{bmatrix} \ddot{x} \\ \ddot{z} \end{bmatrix} = \begin{bmatrix} \Delta F_x \\ \Delta F_z \end{bmatrix} \quad (25)$$

For first iteration initial guess of displacement are made arbitrarily small. In each iteration fluid film thickness is modified due to new position of journal centre which leads to variation in instantaneous forces. Solution is obtained by numerically integration using Runge-Kutta 4th order method with the help of difference between the instantaneous film force and the static equilibrium film force components. For next iterations previous values of positions and velocities serves as initial guess.

I. Critical mass

Critical mass of the system is function of dynamic characteristics of bearing. As per Routh-Hurwitz stability criteria critical mass is calculated by using the stiffness and damping coefficients and is expressed as:

$$\bar{M}_c = \frac{a_0}{b_0 - c_0} \quad (26)$$

$$\text{where } a_0 = \frac{(C_{xx} * C_{yy} - C_{yx} * C_{xy})}{(C_{xx} + C_{yy}) * (K_{xx} * K_{yy} - K_{yx} * K_{xy})}$$

$$b_0 = \frac{(K_{xx} * C_{yy} + C_{xx} * K_{yy} - K_{yx} * C_{xy} - K_{xy} * C_{yx})}{K_{xx} * C_{xx} + C_{yy} * K_{yy} + K_{yx} * C_{xy} + K_{xy} * C_{yx}}$$

$$c_0 = \frac{(C_{xx} + C_{yy})}{(C_{xx} + C_{yy})}$$

If applied journal mass \bar{M}_j is less than the critical mass \bar{M}_c i.e., $\bar{M}_j \leq \bar{M}_c$ the system shows stability converse to this statement if $\bar{M}_j > \bar{M}_c$ then the system shows instability.

However for any negative values of critical mass system always shows stability.

J. Threshold speed

It can be defined as the speed at which rotor becomes unstable. Threshold speed depends upon stiffness and damping coefficient. It can be given as:

$$\bar{\Omega}_s = \sqrt{\frac{\bar{F} * K_{sq}}{\bar{M}_c}} \quad (27)$$

$$\text{where, } K_{sq} = \frac{K_{xx} * C_{zz} + C_{xx} * K_{zz} - K_{zx} * C_{zz} - K_{zz} * C_{zx}}{C_{xx} + C_{zz}}$$

K. Whirl frequency ratio

It is the ratio of the rotor whirl or processional frequency to the rotor onset speed at instability. Whirl frequency ratio (\bar{f}) depends on the dynamic bearing characteristics. Negative value of \bar{f} implies absence of whirl.

$$\bar{f} = \sqrt{\frac{(K_{xx} - K_{sq}) * (K_{yy} - K_{sq}) - K_{yx} * K_{xy}}{(C_{xx} * C_{yy} - C_{yx} * C_{xy})}} \quad (28)$$

L. Mass Reduction Factor

When journal mass is kept equal to critical mass ($\bar{M}_j = \bar{M}_c$) the linear equations predicts limit cycle whereas nonlinear equations predicts instability of system by journal moving away from equilibrium position due to excessive journal mass. Hence to make system stable journal mass required to

be reduced and the factor by which journal mass is reduced is known as mass reduction factor. Mathematically it is given as:

$$\text{Mass reduction factor } (\bar{M}_r) = \frac{\text{Reduced journal mass}}{\text{Critical mass of journal } (\bar{M}_c)} \quad (29)$$

III. SOLUTION PROCEDURE

The theoretical prediction of hydrodynamic pressures in the bearing is obtained by the solution of modified Reynolds equation satisfying the appropriate boundary conditions. The steady state and dynamic pressure profile is obtained easily by finite difference techniques these are based upon the approximations that permit replacing differential equations by finite difference equations. These approximations are algebraic in form, and the solutions are related to grid points.

Rewriting modified Reynolds equation for couple stress fluid Equation (4.17):

$$\frac{\partial}{\partial \theta} \left(f(\bar{l}, \bar{h}) \frac{\partial \bar{p}}{\partial \theta} \right) + \frac{\partial}{\partial \bar{z}} \left(f(\bar{l}, \bar{h}) \frac{\partial \bar{p}}{\partial \bar{z}} \right) = 6 \frac{\partial \bar{h}}{\partial \theta} \quad (30)$$

$$\text{Where, } f(\bar{l}, \bar{h}) = \bar{h}^3 - 12\bar{h}\bar{l}^2 + 24\bar{l}^3 \tanh\left(\frac{\bar{h}}{2\bar{l}}\right)$$

The fluid film domain is discretized. Discretized fluid film contains uniform mesh size. Refined mesh is used for the analysis. Refined mesh is optimum mesh size at which result obtained does not vary considerably as compared to the results obtained by further refining mesh size. Excessive refinement causes too long computational time hence optimum mesh size is selected. By using FDM we can derive general governing equation for pressure distribution along horizontal and vertical axis and for variation of fluid film thickness within fluid dim domain. The optimum number of nodes considered for present analysis is 25921.

General equation for pressure gradient along horizontal direction:

$$\frac{\partial}{\partial \theta} \left(f(\bar{l}, \bar{h}) \frac{\partial \bar{p}}{\partial \theta} \right) = \frac{[(f(\bar{l}, \bar{h})_{i,j} + f(\bar{l}, \bar{h})_{i+1,j})(\bar{p}_{i+1,j} - \bar{p}_{i,j}) - (f(\bar{l}, \bar{h})_{i,j} + f(\bar{l}, \bar{h})_{i-1,j})(\bar{p}_{i,j} - \bar{p}_{i-1,j})]}{2\Delta\theta^2} \quad (31)$$

where i and j represents x and y coordinate of nodes in film domain. Similarly general equation for pressure gradient along vertical direction:

$$\frac{\partial}{\partial \bar{z}} \left(f(\bar{l}, \bar{h}) \frac{\partial \bar{p}}{\partial \bar{z}} \right) = \frac{[(f(\bar{l}, \bar{h})_{i,j} + f(\bar{l}, \bar{h})_{i+1,j})(\bar{p}_{i+1,j} - \bar{p}_{i,j}) - (f(\bar{l}, \bar{h})_{i,j} + f(\bar{l}, \bar{h})_{i-1,j})(\bar{p}_{i,j} - \bar{p}_{i-1,j})]}{2\Delta\bar{z}^2} \quad (32)$$

General equation for film thickness gradient within film domain:

$$6U \frac{\partial \bar{h}}{\partial \theta} = 6U \left[\frac{\bar{h}_{i+1} - \bar{h}_i}{\theta_{i+1} - \theta_i} \right] \quad (33)$$

Pressure at a node can be predicted by solving equation (30) on using equations (31), (32) and (33).

For 'n' number of nodes we get 'n' number of equations. These equations are solved simultaneously by using suitable numerical method. In the present analysis modified Reynolds equation (34) is solved simultaneously by using

PDE toolbox (Partial Differential Equation toolbox) of MATLAB software. The simultaneous solution of these equations gives pressure distribution over fluid film.

Fluid film domain is selected by applying following boundary conditions the following boundary conditions to the flow field. Ambient pressure is assumed to be zero.

$$\bar{p} = 0 \text{ at } \theta = 0, \theta_2 \tag{34}$$

$$\bar{p} = 0 \text{ at } \bar{z} = 0, 2 \tag{35}$$

$$\frac{\partial \bar{p}}{\partial \theta} = 0 \text{ at } \theta = \theta_2 \tag{36}$$

IV. RESULT

Results are obtained for the analysis of plain circular bearing characteristics lubricated with couple stress fluid with varying couple stress parameter from 0 to 0.5 with the step of 0.1. The effect of eccentricity ratio is also considered by varying it from 0.3 to 0.7 with step size of 0.1.

A. Effect of eccentricity ratios ($\bar{\epsilon}$) and couple stress parameters (\bar{l}) on attitude angle (ϕ)

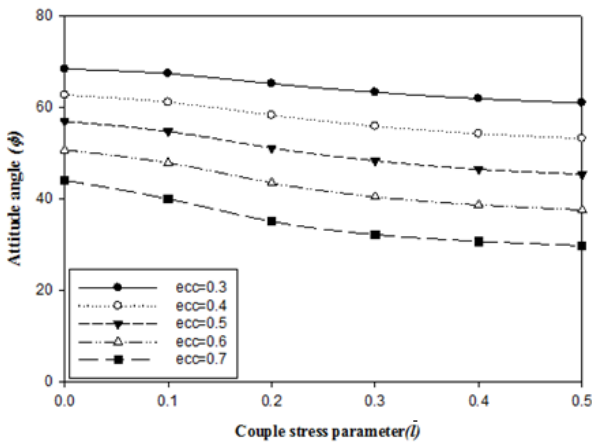


Fig. 2 Attitude angle (ϕ) Vs Couple stress parameters (\bar{l})

From graphs it is clear that attitude angle goes on decreasing as the eccentricity ratio increases hence there exists inverse relation between attitude angle and eccentricity ratio. As per the definition of attitude angle it is angle between load and line of centre. Hence for almost vertical load attitude angle measures lower value whereas its value goes on increasing as the load moves away from vertical direction.

B. Effect of eccentricity ratios ($\bar{\epsilon}$) and couple stress parameters (\bar{l}) on bearing load (\bar{F})

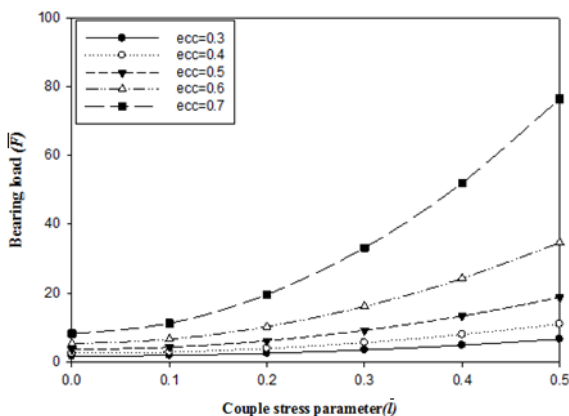


Fig.3 Bearing load (\bar{F}) Vs Couple stress parameters (\bar{l})

With the help of nature of graphs it is clear that bearing load goes on increasing as the eccentricity ratio increases hence there exists symmetric relation between bearing load and eccentricity ratio. It is also observed that margin through which bearing load increases goes on increasing as the eccentricity ratio increases. Considering the effect of couple stress fluid on bearing load, significant effect is observed for the system operating at various eccentricity ratios. At particular eccentricity ratio bearing load goes on increasing as the couple stress parameter increases.

C. Effect of eccentricity ratios ($\bar{\epsilon}$) and couple stress parameters (\bar{l}) on stiffness coefficient (\bar{K}_{xx})

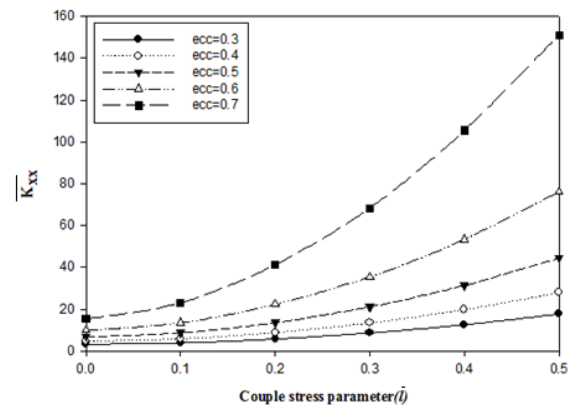


Fig. 4 Stiffness coefficient (\bar{K}_{xx}) Vs Couple stress parameters (\bar{l})

With the help of nature of graphs it is clear that stiffness coefficient (\bar{K}_{xx}) goes on increasing as the eccentricity ratio increases hence there exists symmetric relation between stiffness coefficient (\bar{K}_{xx}) and eccentricity ratio. It is also observed that margin through which stiffness coefficient (\bar{K}_{xx}) goes on increasing as the eccentricity ratio increases. Consider the system lubricated with couple stress fluid and operating at different eccentricity ratios. From the Figure (7.3) it is seen that at particular eccentricity ratio stiffness coefficient (\bar{K}_{xx}) goes on increasing as the couple stress parameter increases.

D. Effect of eccentricity ratios ($\bar{\epsilon}$) and couple stress parameters (\bar{l}) on stiffness coefficient (\bar{K}_{xz})

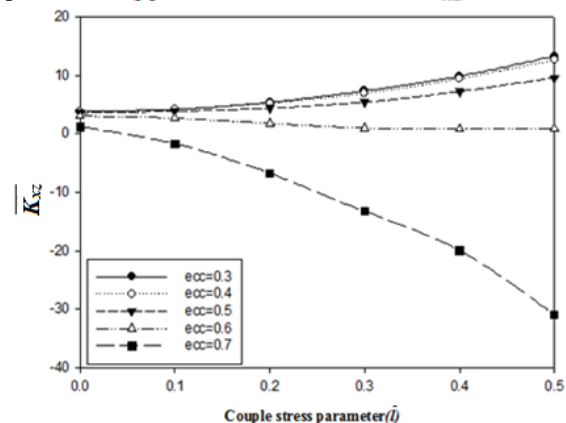


Fig.5 Stiffness coefficient (\bar{K}_{xz}) Vs Couple stress parameters (\bar{l})

With the help of nature of graphs it is conclude that stiffness coefficient (\bar{K}_{xz}) goes on decreasing as the eccentricity ratio increases hence there exists inverse relation between stiffness coefficient (\bar{K}_{xz}) and eccentricity ratio. It is also observed that margin through which stiffness coefficient (\bar{K}_{xz}) varies goes on increasing as the eccentricity ratio increases.

E. Effect of eccentricity ratios ($\bar{\epsilon}$) and couple stress parameters (\bar{l}) on stiffness coefficient (\bar{K}_{zx})

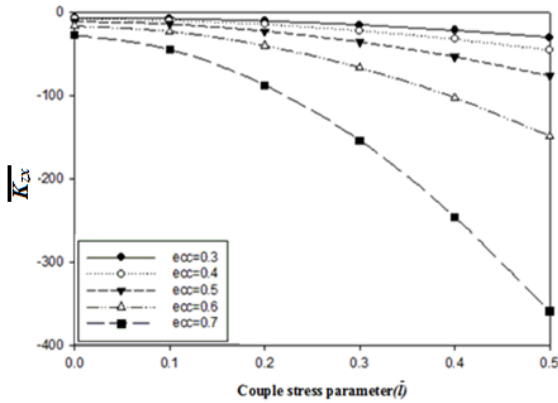


Fig. 6 Stiffness coefficient (\bar{K}_{zx}) Vs Couple stress parameters (\bar{l})

With the help of nature of graphs it is clear that stiffness coefficient (\bar{K}_{zx}) goes on decreasing as the eccentricity ratio increases hence there exists inverse relation between stiffness coefficient (\bar{K}_{zx}) and eccentricity ratio. It is also seen that margin through which stiffness coefficient (\bar{K}_{zx}) varies goes on increasing as the eccentricity ratio increases. Considering couple stress fluid as lubricant for the system operating at various eccentricity ratios. Stiffness coefficient (\bar{K}_{zx}) is influenced by couple stress parameter at particular eccentricity ratio stiffness coefficient (\bar{K}_{zx}) goes on decreasing as the couple stress parameter increases.

F. Effect of eccentricity ratios ($\bar{\epsilon}$) and couple stress parameters (\bar{l}) on stiffness coefficient (\bar{K}_{zz})

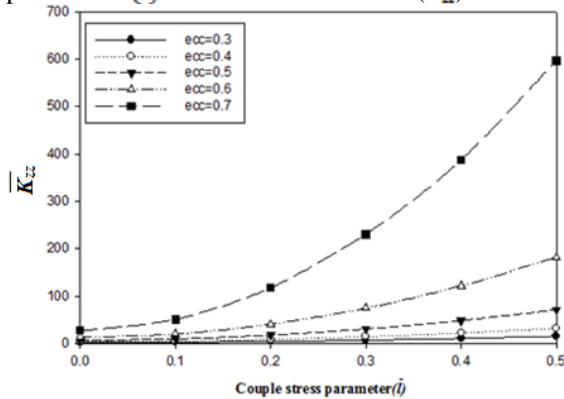


Fig. 7 Stiffness coefficient (\bar{K}_{zz}) Vs Couple stress parameters (\bar{l})

With the help of nature of graphs it is clear that stiffness coefficient (\bar{K}_{zz}) goes on increasing as the eccentricity ratio increases hence there exists symmetric relation between stiffness coefficient (\bar{K}_{zz}) and eccentricity ratio. Analysis shows that margin through which stiffness coefficient (\bar{K}_{zz}) changes goes on increasing as the eccentricity ratio increases. Consider the system lubricated with couple stress fluid influence of couple stress parameter is observed on stiffness coefficient. At particular eccentricity ratio stiffness coefficient (\bar{K}_{zz}) goes on increasing as the couple stress parameter increases.

G. Effect of eccentricity ratios ($\bar{\epsilon}$) and couple stress parameters (\bar{l}) on damping coefficient (\bar{C}_{xx})

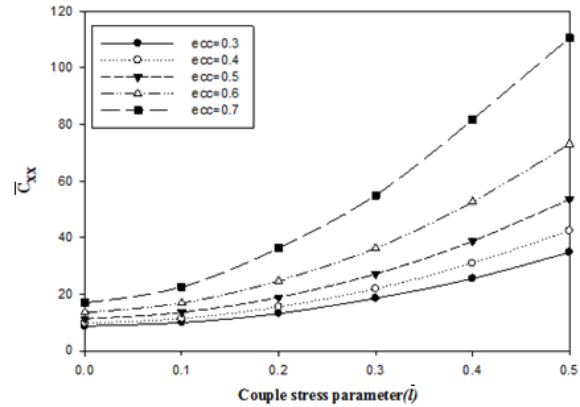


Fig. 8: Damping coefficient (\bar{C}_{xx}) Vs Couple stress parameters (\bar{l})

With the help of nature of graphs it is clear that damping coefficient (\bar{C}_{xx}) goes on increasing as the eccentricity ratio increases hence there exists symmetric relation between damping coefficient (\bar{C}_{xx}) and eccentricity ratio for Newtonian fluid. The studies also shows that margin through which damping coefficient (\bar{C}_{xx}) changes goes on increasing as the eccentricity ratio increases.

H. Effect of eccentricity ratios ($\bar{\epsilon}$) and couple stress parameters (\bar{l}) on damping coefficient ($\bar{C}_{xz} \sim \bar{C}_{zx}$)

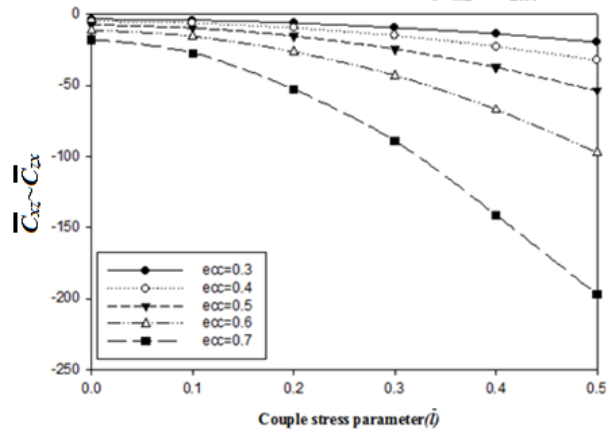


Fig. 9 damping coefficients ($\bar{C}_{xz} \sim \bar{C}_{zx}$) Vs Couple stress parameters (\bar{l})

With the help of graph damping coefficient (\bar{C}_{xz}) and (\bar{C}_{zx}) decreases as the eccentricity ratio increases. Considering the values obtained at various eccentricity ratios it can be stated that the margin through which damping coefficient (\bar{C}_{xz}) and (\bar{C}_{zx}) vary goes on increasing as the eccentricity ratio increases.

I. Effect of eccentricity ratios ($\bar{\epsilon}$) and couple stress parameters (\bar{l}) on damping coefficient (\bar{C}_{zz})

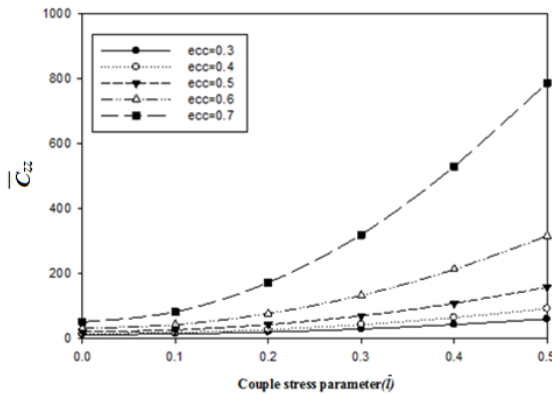


Fig. 10: Damping coefficient ($\overline{C_{zz}}$) Vs Couple stress parameters (\overline{l})

From graph it is clear that damping coefficient ($\overline{C_{zz}}$) goes on increasing as the eccentricity ratio increases hence there exists symmetric relation between damping coefficient ($\overline{C_{zz}}$) and eccentricity ratio. It is also seen that margin through which damping coefficient ($\overline{C_{zz}}$) increases goes on increasing as the eccentricity ratio increases. Effect of couple stress fluid is observed on damping coefficient. Obtained results shows that at any particular eccentricity ratio damping coefficient ($\overline{C_{zz}}$) goes on increasing as the couple stress parameter increases. In case of couple stress fluid it is seen that margin through which damping coefficient ($\overline{C_{zz}}$) changes goes on increasing as the eccentricity ratio increases.

J. Effect of eccentricity ratios ($\overline{\epsilon}$) and couple stress parameters (\overline{l}) on critical mass ($\overline{M_c}$)

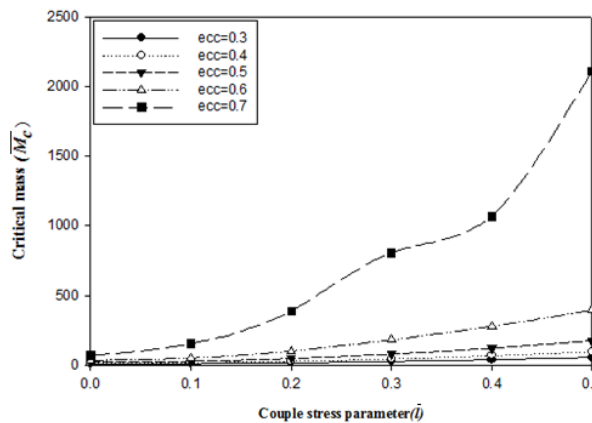


Fig. 11: Critical mass ($\overline{M_c}$) Vs Couple stress parameters (\overline{l})

With the help of nature of graphs it is clear that critical mass goes on increasing as the eccentricity ratio increases. For the system lubricated with couple stress fluid it is seen that critical mass is influenced by couple stress parameter. At particular eccentricity ratio critical mass goes on increasing as the couple stress parameter increases. For couple stress fluid margin through which critical mass goes on increasing as the eccentricity ratio increases.

K. Effect of eccentricity ratios ($\overline{\epsilon}$) and couple stress parameters (\overline{l}) on Threshold speed ($\overline{\Omega_s}$)

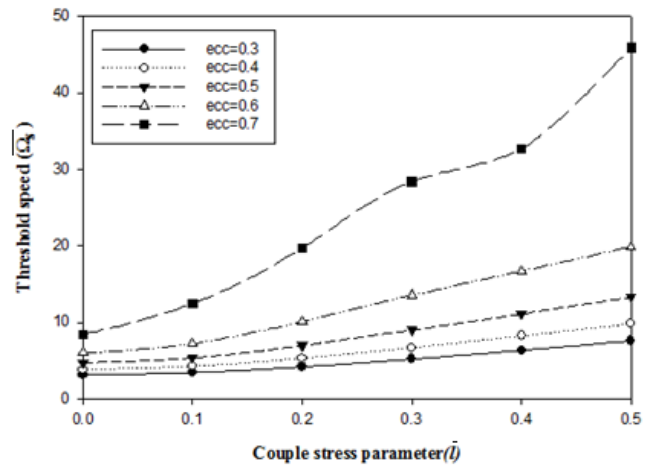


Fig. 12 Threshold speed ($\overline{\Omega_s}$) Vs Couple stress parameters (\overline{l})

The result shows that threshold speed goes on increasing gradually with increase in couple stress parameter. Hence couple stress parameter allows system to operate at higher speed. System shows stability with highest speed operating under higher couple stress parameter and higher eccentricity ratio. For couple stress fluid also it is observed that margin through which threshold speed goes on increasing as the eccentricity ratio increases.

L. Effect of eccentricity ratios ($\overline{\epsilon}$) and couple stress parameters (\overline{l}) on Whirl frequency ratio (\overline{f})

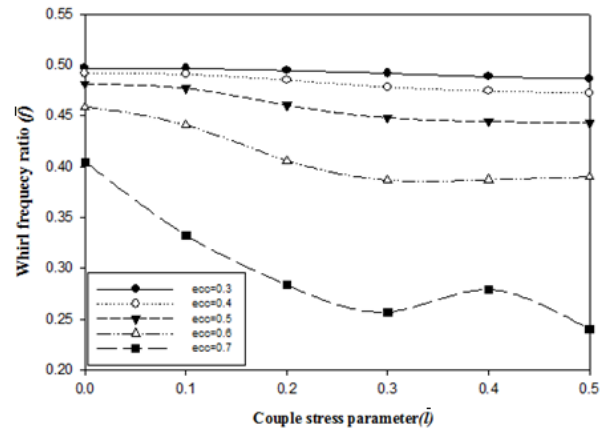


Fig. 13 Whirl frequency ratio (\overline{f}) Vs Couple stress parameters (\overline{l})

Whirl frequency goes on decreasing with increase in couple stress parameter however at eccentricity ratio 0.7 it is found that whirl frequency initially decreases up to $\overline{l} = 0.3$ and value observed is 0.2566 whereas $\overline{l} = 0.4$ it is observed increased value of 0.2791 and again at $\overline{l} = 0.5$ it falls down to 0.2403. Hence dramatic variation in whirl frequency ratio is observed when system is operated at higher eccentricity ratios.

V. CONCLUSIONS

On the basis of linear and nonlinear analysis of plain bearing lubricated with couple stress fluid following conclusion are drawn:

1. Strong influence of couple stress fluid is observed on the static and dynamic characteristics of bearing.
2. Stability margin of bearings increases with increase in couple stress parameter.

3. At particular eccentricity bearing load and critical mass of the system increases with increase in couple stress parameter while attitude angle decreases.
4. Couple stress parameter allows the system to run at higher speed by improving threshold speed limits and reducing whirl frequency ratio of rotor.
5. Linear study predicts limit cycle at critical mass of journal while for the same mass nonlinear study predicts instability of system hence linear study shows better stability margin as compared to nonlinear study operating under same conditions.
6. The peak to peak orbit amplitude increases with either increase in eccentricity ratio or increases couple stress parameter. Hence maximum peak to peak orbit amplitude is observed at higher eccentricity ratio and higher couple stress parameter.
7. Mass reduction factor goes on decreasing as couple stress parameter or eccentricity ratio or both increases.
8. Margin through which mass reduction ratio decreases goes on increasing with increase in either couple stress parameter or eccentricity ratio or both.

ACKNOWLEDGEMENT

The author would like to thank for the valuable suggestions and guidance given by Dr.L.G.Navale, Prof.Mahesh Jidaji. And special thanks to Dr.K.K.Dhande (HOD-Mechanical engineering) and Dr.R.K.Jain (Principal)for their support to complete this assignment.

REFERENCES

- [1] G. Ramanaiah and Priti Sarkar "Squeeze films and thrust bearings lubricated by fluids with couple stress". *Wear* 48 (1978) pp. no: - 309 – 316.
- [2] G. Ramanaiah and Priti Sarkar "Slider bearings lubricated by fluids with couple stress". *Wear* 52 (1979) pp. no: - 27 –36.
- [3] Chandan Singh "Lubrication theory for couple stress fluids and its application to short bearings". *Wear* 80 (1982) pp. no: - 281- 290.
- [4] R. S. Gupta and L. G. Sharma "Analysis of couple stress lubricant in hydrostatic thrust bearing". *Wear* 125 (1988) pp. no: - 257 – 269.
- [5] R. Sinhasan and K. C. Goyal "Elastohydrodynamic studies of circular journal bearings with non-Newtonian lubricants". *Tribology International* (1990) Vol 23 No 6 pp. no: -419-428.
- [6] R. Sinhasan and K. C. Goyal "Transient response of a circular journal bearing lubricated with non-Newtonian lubricants". *Wear* 156 (1992) pp. no: - 385-399.
- [7] J. R. Lin "Effects of couple stresses on the lubrication of finite journal bearings". *Wear* 206 (1997) Pg no: -171–178.
- [8] J. R. Lin "Squeeze film characteristics of finite journal bearings: couple stress fluid model". *Tribology International* Vol 31(1998) No 4 pp. no: - 201–207.
- [9] J. R. Lin "Linear stability analysis of rotor-bearing system: couple stress fluid model". *Computers and Structures* 79 (2001) pp. no: - 801-809.
- [10] J. R. Lin, R. F. Lu and T. B. Chang "Derivation of dynamic couple-stress Reynolds equation of sliding squeezing surfaces and numerical solution of plane inclined slider bearings". *Tribology International* 36 (2003) pp. no: - 679–685.
- [11] Xiao-Li Wang, Ke-Qin Zhu and Shi-Zhu Wen "The performance of dynamically loaded journal bearings lubricated with couple stress fluids". *Tribology International* 35 (2002) pp. no: -185–191.
- [12] Hsiu-Lu Chiang, Cheng-Hsing Hsu and Jaw-Ren Lin "Lubrication performance of finite journal bearings considering effects of couple stresses and surface roughness". *Tribology International* 37 (2004) pp. no: - 297-303.
- [13] N. B. Naduvinamani and S.B. Patil "Numerical solution of finite modified Reynolds equation for couple stress squeeze film lubrication of porous journal bearings". *Computers and Structures* 87 (2009) pp. no: - 1287–1295.
- [14] Matthew Cha, Evgeny Kuznetsov and Sergei Glavatskih "A comparative linear and nonlinear dynamic analysis of compliant cylindrical journal bearings". *Mechanism and Machine Theory* 64 (2013) pp. no: - 80–92.
- [15] A. A. Elsharkawy and L. H. Guedouar "An inverse solution for finite journal bearings lubricated with couple stress fluids". *Tribology International* 34 (2001) pp. no: - 107–118.
- [16] Chapter 5, "Static characteristics of journal bearings". *Tribology Series* Vol. 33 (1997) pp. no: -114.